Formation of Al_2O_3 supported Ni_2P based 3D catalyst for atmospheric deoxygenation of rubberwood sawdust

Pranshu Shrivastava*

Thammasat University Research Unit in Bioenergy and Catalysis, Thammasat University, Klongluang, Pathumthani, Thailand-12120

Abstract. An ex-situ gravitational fixed bed pyrolysis reactor was used over Al_2O_3 supported Ni_2P based catalyst with various Ni/P molar ratios (0.5-2.0) and constant nickel loading of 5.37 mmol/g Al_2O_3 to determine the hydrodeoxygenation of rubberwood sawdust (RWS) at atmospheric pressure. The 3D catalysts formed were characterized structurally as well as acidic properties were determined by hydrogen-temperature programmed reduction (TPR). The Ni_2P phase formed completely on Al_2O_3 for 1.5 Ni/P ratio, although lesser crystallite sizes of Ni_2P were seen at Ni/P ratios less than 1.5. Additionally, it was shown that when nickel loading level increased, acidity increased and specific surface area dropped, probably because nickel phosphate is not easily converted to Ni_2P. When Ni/P ratio was 1.5, Ni_2P phase fully formed on Al_2O_3. The catalytic activity was explained in terms of impacts of reaction temperature and Ni/P molar ratio. At relatively high temperature of 450°C, the high-value deoxygenated produce was predominantly composed of n-alkanes. Based on the findings, it was suggested that hydrogenolysis, hydrodeoxygenation, dehydration, decarbonylation, and hydrogenation are all part of mechanism underlying hydrotreatment of RWS. In conclusion, the synthesized Ni_2P/Al_2O_3 catalyst was capable of deoxygenating RWS with ease at atmospheric pressure, primarily resulting in long chained (C_9-C_{24}) hydrocarbons and acetic acid.

Keywords: 3D catalyst; catalytic pyrolysis; hydrodeoxygenation; nickel phosphide; rubberwood sawdust

1. Introduction

The world's nonrenewable fossil fuel supplies are currently being depleted because of rising energy consumption brought on by advances in technology, global economic growth, and population growth. This has led to substantial increases in the price of petroleum. These elements may cause an energy shortage while simultaneously hastening climate change. In light of this, renewable alternatives to fossil fuels have been suggested, including biofuels, which are fuels made from biomass and wastes. Due to its sustainable renewability, moderate synthesis conditions, and lack of negative effects on other industries, the second-generation biofuel biodiesel made from rubberwood sawdust (RWS) has the greatest potential to replace fossil diesel (Shrivastava *et al.* 2021). However, due to the presence of oxygenates, especially carboxyl compounds, it hasn't been utilized directly as a commercial fuel because of its low calorific value, high viscosity, and low stability. Consequently, it needs a second procedure involving catalytic hydrodeoxygenation (HDO)

---

*Corresponding author, Ph.D., E-mail: shri.pranshu@gmail.com

(Zulkepli *et al.* 2018).

As a catalyst for the HDO reaction, nickel phosphide has been employed because it is affordable, has a high catalytic performance for hydrotreatment processes including hydrodesulfurization and hydrodenitrogenation, and even has a long lifespan (Xin *et al.* 2016). The bifunctional active sites in Ni_2P (one of the several nickel phosphide compounds) are another feature (Cecilia *et al.* 2016). During HDO reactions, Ni_2P as a catalyst operates just as well as the noble metals, such as platinum and palladium (Prins and Bussell 2012). Furthermore, during the HDO of methyl laurate, Ni_2P/SiO_2 showed strong selectivity for n-C_{11} and n-C_{12} (Chen *et al.* 2020). Additionally, it was discovered that bulk Ni_2P and Ni_2P supported on γ-Al_2O_3 were appropriate catalysts for the production of pentadecane (C_{16}) by decarbonylation and decarboxylation during the HDO of palmitic acid (Peroni *et al.* 2016). However, little research has been done on the HDO of complicated feedstocks like RWS. Additionally, the majority of HDO reactions have been carried out in harsh settings including those with high pressures (Santillan-Jimenez *et al.* 2018). In order to lower the cost of the necessary equipment, HDO at atmospheric pressure needs to be studied. Additionally, the procedure would be safer.

This study looked into the HDO of WCO and the catalytic activity of Ni_2P at atmospheric pressure. The catalyst was supported by alumina oxide (Al_2O_3), and Ni_2P was created by phosphidizing nickel phosphate. The scientific theory of "green carbon" is consistent with the efficient use of both RWS and biochar (Shrivastava *et al.* 2021).

2. Material and methods

2.1 Catalyst preparation

2.1.1 Ni2P/Al2O3 catalysts synthesis

Temperature programme reduction (TPR) was used for preparation of Ni_2P/Al_2O_3 catalyst samples. First, a mixture of $(NH_4)_2HPO_4$ and $Ni(NO_3)_2.6H_2O$ was wet-impregnated into 1 g of Al_2O_3 at various Ni/P molar ratios for different fractions ranging from 0.5 - 2.0 and Ni (5.37 mmol Ni/g Al_2O_3). The catalyst samples were then aged for 12 hours at room temperature, dried for 12 hours at 110°C, and then calcined and reduced in one step for 4 hours at 600°C with a heating rate of 5 °C per minute while being supplied with a 40 mL/min hydrogen (H_2) flow. After being cooled to the proper reaction temperature, the reduced catalyst samples were then assessed appropriate for RWS deoxygenation. The samples were subsequently passed for an additional 4 hours in N_2 environment for characterization. Different samples are labelled "5.37-Ni_2P/ Al_2O_3-x-TPR," where "x" denotes molar ratio of Ni/P, and "TPR" denotes Ni_2P preparation technique.

2.1.2 Ni2P/Al2O3 catalysts characterization

The structures of catalyst samples were discovered by powder X-ray diffraction (XRD) studies. The measurements were carried out using a Cu-Kα X-ray source with a wavelength of 1.54 (X'Pert, Philips). The scans were carried out for the range of 20-80 ° using a step size of 0.02° min^{-1}, and radiation was generated at 40 kV and 20 mA. Scherrer's equation was used to calculate the crystallite sizes. By using H_2- TPR in a quartz reactor to load 0.1 g of the test catalyst in the presence of 5 percent (v/v) H_2 in N_2 at a flow rate of 30 mL/min and heat the sample from 100 to 900°C at 10°C per minute, the reducibility of each catalyst sample was examined (Zhao *et al.* 2020). A thermal conductivity detector was used to calculate the H_2 consumption rate. Using a
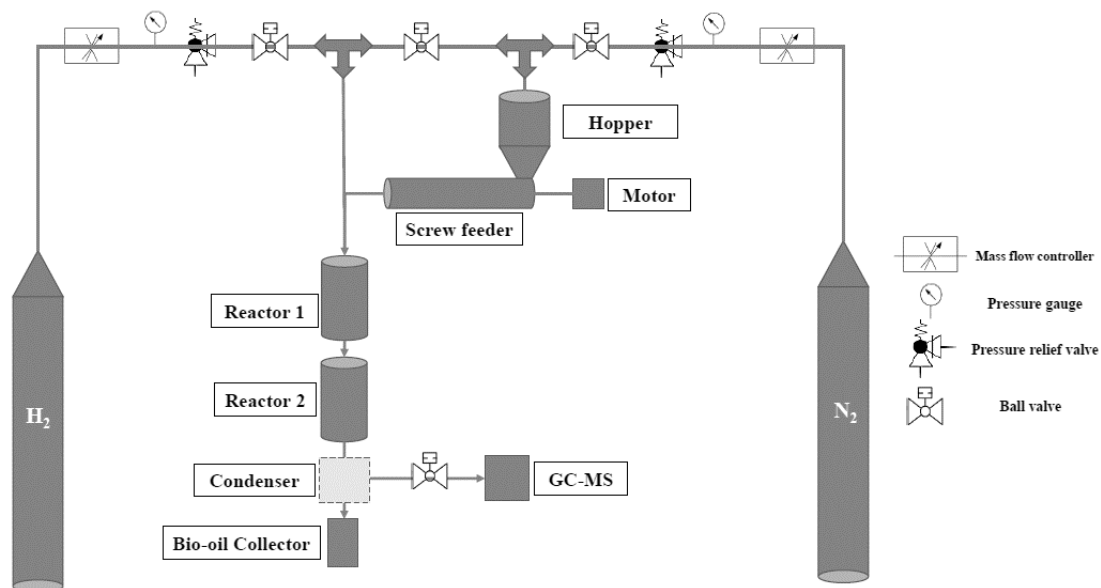
Fig. 1 Schematic Diagram of the process

TPD/R/O100a, ammonia (NH$_3$)-temperature programmed desorption (TPD) was used to characterize the acidic characteristics. Over a temperature range of 100 to 500°C, the quantity of desorbed NH$_3$ was correlated with number of acid sites. The BET method was used to determine specific surface areas of Ni$_2$P/Al$_2$O$_3$ samples. The samples underwent a pretreatment to get rid of any moisture before being allowed to adsorb N$_2$ at -196°C.

2.2 Catalytic pyrolysis

Reactor 1 with a bed capacity of 15.6 cm^3 was filled with the Ni$_2$P/Al$_2$O$_3$ catalyst under test (4 ± 0.01 g). The catalyst was subsequently decreased for 1 hour at 600 °C and 20 mL/min of H$_2$. The catalyst was utilized for HDO of RWS at atmospheric pressure in a tubular fixed-bed reactor 2 after reduction process was finished and catalyst had been chilled to appropriate reaction temperature (schematic shown in Fig.1). Physicochemical properties of the RWS used in study are displayed in Table 1. The N$_2$ gas, flowed at 50 mL/min. Based on GC-MS measurements, following was estimated to determine the oxygen removal rate:

$$\text{Oxygen Removal} = \left[\frac{T_{feed} - T_{product}}{T_{feed}}\right] \text{X } 100$$

where T$_{feed}$ and T$_{product}$ are contents found in RWS sample respectively and its liquid products as determined by GC-MS studies.

The reaction temperature used for the pyrolysis of RWS in the range of 400 to 500°C. A GC system (Shimadzu, GC-8A) outfitted with a packed ShinCarbon 80/100 column, and a thermal conductivity detector was also used to identify the gaseous products. All three temperatures — injection temperature, initial temperature, and final temperature — were maintained at 50°C.

Table 1 Physicochemical Characterization of RWS

Properties	RWS
Proximate Analysis	
Moisture content (wt.%, wet basis)	6.57±0.05
Volatile matter (wt.%, dry basis)	74.84±0.18
Fixed carbon (wt.%, dry basis)	17.53±0.19
Ash (wt.%, dry basis)	1.06±0.03
Lignocellulosic content (wt.%, dry basis)	
Cellulose	58.45±0.27
Hemicellulose	16.24±0.41
Lignin	14.26±0.13
Extractives	11.05±0.17
Ultimate Analysis (wt.%, dry basis)	
Carbon (C)	48.56±0.17
Hydrogen (H)	5.97±0.02
Nitrogen (N)	0.29±0.01
Oxygen (O)*	45.17±0.13
Sulphur (S)	0.01±0.01
Elemental composition (mg/kg)	
Silicon (Si)	2479
Iron (Fe)	178.4
Calcium (Ca)	4268
Magnesium (Mg)	997
Sodium (Na)	64.5
Potassium (K)	5014
Higher heating values and lower heating values (MJ/kg)	
HHV	25.92±0.16
LHV	21.34±0.32
Other properties	
Molecular formula	$CH_{1.547}O_{0.841}$
H/C ratio	1.59
O/C ratio	0.69
Bulk density (kg/m³)	305.58±0.38

3. Results and discussions

3.1 Characterization of Ni₂P/Al₂O₃

Fig. 2 represents reducibility of Ni_2P/Al_2O_3 was examined by using H_2-TPR analysis. Ni_2P catalyst precursors are co-impregnated to form phosphate groups on the Al_2O_3 surface which leads
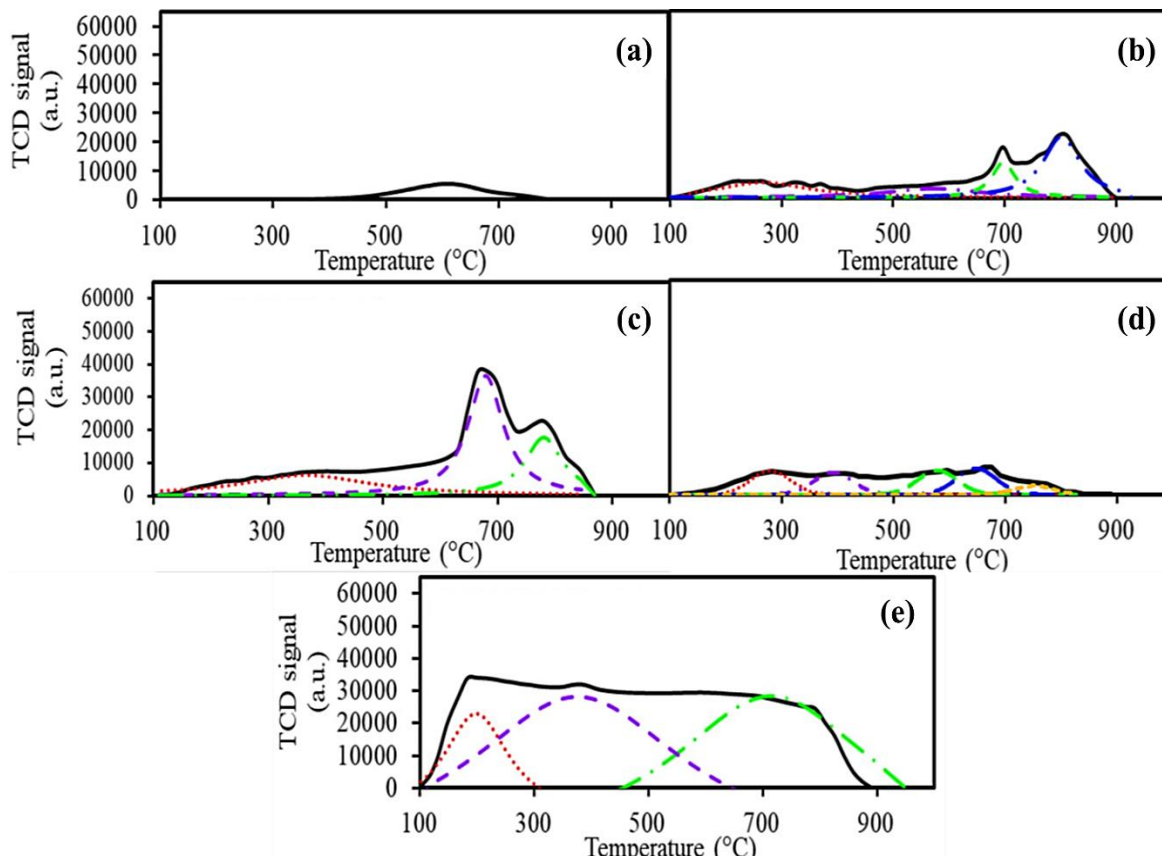
Fig. 2 H₂ TPR profiles of Ni₂P/Al₂O₃ catalyst samples

to phosphidation in each stage during reduction reaction. Due to the simultaneous production of H_2O and PH_3, TPR curve for nickel phosphide as a catalyst is more complex when it is used for reduction. The peak was associated with hygroscopic precursor reduction, which resulted in breakdown of salts containing nitrogen at temperatures between 100 and 300°C. The wide reduction peak could be broken down into three separate peaks at temperatures between 300 & 400°C, 400 & 700°C, and 700 & 900°C, respectively. These peaks pertained to reduction of nickel oxide, nickel oxy-phosphates [$Ni_2P_4O_{12}$, $Ni_2P_2O_7$, and $Ni(PO_3)_2$], and nickel phosphate, respectively.

Fig. 3 also displays NH₃-TPD profiles of Ni₂P/Al₂O₃ catalyst samples with various Ni loading levels. Only two separate peaks were found in the Ni₂P/Al₂O₃ with modest Ni levels (1.16 and 5.37 mmol/g Al₂O₃) and attributed to Ni₂P acid sites and nickel-rich phosphide ($Ni_{12}P_5$). With an increase in Ni loading level, the samples' overall acidity increased (see Table 2).

3.2 Pyrolysis product distribution

Fig. 4 represents the product distribution of catalytic pyrolysis of RWS. The maximum output
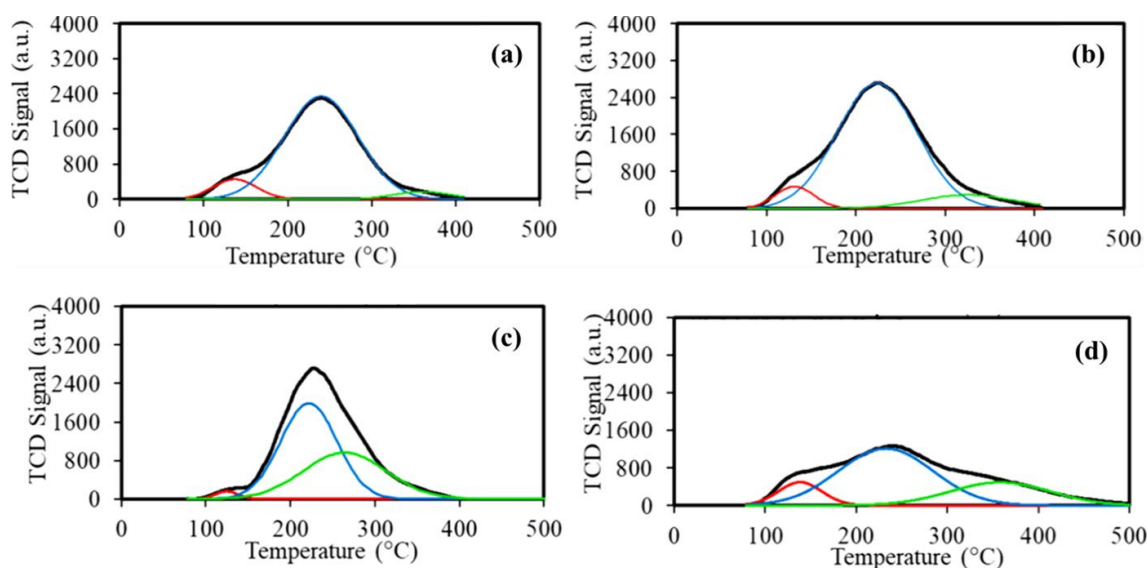
Fig. 1 NH$_3$ TPD profiles of Ni$_2$P/Al$_2$O$_3$ catalyst samples

Table 2 Physicochemical properties of catalyst used

Catalyst[x]	Acidic properties			Total acidity (mmol/g)	Crystallite size of Ni$_2$P (nm)[y]	S$_{BET}$ (m^2/g)
	Peak Temperature °C					
	180-200	200-220	220-240			
Fresh 5.37-Ni$_2$P/Al$_2$O$_3$-0.5	0.08	0.84	n.d.	0.87	21.9	236
Spent 5.37-Ni$_2$P/Al$_2$O$_3$-0.5					0.1	< 0.1
Fresh 5.37-Ni$_2$P/Al$_2$O$_3$-1.0	0.04	1.24	< 0.1	1.27	25.8	474
Spent 5.37-Ni$_2$P/Al$_2$O$_3$-1.0					26.4	0.1
Fresh 5.37-Ni$_2$P/Al$_2$O$_3$-1.5	0.11	1.37	n.d.	1.40	31.8	576
Spent 5.37-Ni$_2$P/Al$_2$O$_3$-1.5					33.2	< 0.1
Fresh 5.37-Ni$_2$P/Al$_2$O$_3$-2.0	0.17	0.97	< 0.1	1.01	39.4	403
Spent 5.37-Ni$_2$P/Al$_2$O$_3$-2.0					42.5	0.1

n.d. = not detected
[x] = spend catalyst analyzed at 450 °C after HDO of RWS (P = 1atm)
[y] = XRD is used to determine crystallite sizes

for liquid product (65.2 wt. %) is at 450°C with the catalyst 5.37-Ni$_2$P/Al$_2$O$_3$-1.5 with reaction time of 40 minutes. The distribution of liquid product is maximum at 450 °C and less on the other two temperatures for all reaction time used in this study. The 1.5 ratio of Ni/P displayed a separate peak in its XRD spectrum that was associated to Ni$_2$P phase, indicating strong hydrocarbon selectivity. The triglycerides produced intermediate compounds such aldehydes, ketones, and alcohols when they were subjected to hydrogenolysis. Alkenes were created by further dehydrating these intermediate chemicals. However, n-alkanes were produced since the hydrogenation process took place in an H$_2$ atmosphere. Acid anhydrides, the primary component, are most likely formed

Table 3 Product distribution after catalytic pyrolysis

Catalyst	Hydrocarbon in liquid product (%)							$CO/(CO+CO_2)$ (%)
	n-Alkane $(C_{11}-C_{14})$	n-Alkane $(C_{15}-C_{19})$	n-Alkane $(C_{20}-C_{22})$	n-Alkene	Branched alkane	Cyclic compound	Aromatic hydrocarbon	
5.37-Ni₂P/Al₂O₃-0.5	0.0	0.0	0.2	0.3	0.1	97.3	0.0	0.06
5.37-Ni₂P/Al₂O₃-1.0	0.0	1.6	2.8	0.8	7.4	54.2	0.7	1.0
5.37-Ni₂P/Al₂O₃-1.5	1.6	24.8	31.4	12.6	12.1	7.6	0.8	1.0
5.37-Ni₂P/Al₂O₃-2.0	0.3	13.8	22.7	9.5	14.3	4.7	0.3	0.02

Pyrolysis reaction temperature = 450°C
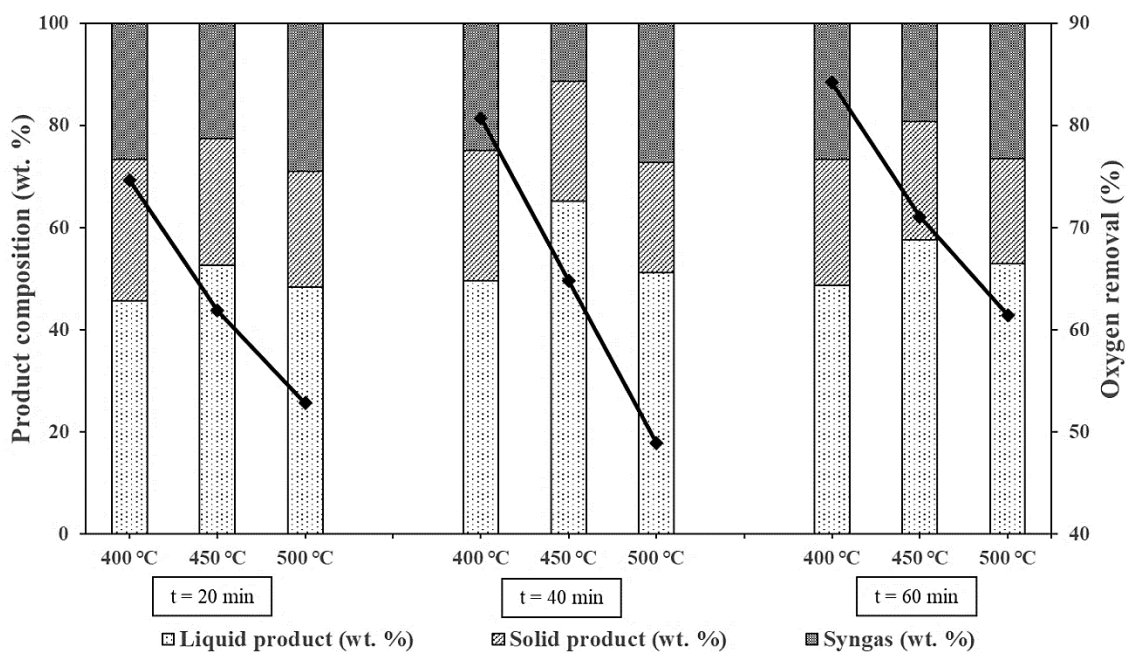
Fig. 2 Product distribution of catalytic pyrolysis of RWS

by various methods. Acid anhydrides are decarbonylated to remove the oxygen. The predominant hydrocarbons were n-alkanes, with trace amounts of cyclic hydrocarbons including aromatic and cycloalkane molecules (refer Table 3). This revealed that only a small number of undesirable routes were involved in deoxygenation reaction.

4. Conclusions

Various Ni₂P/Al₂O₃ catalyst samples were used to successfully catalyze deoxygenation of RWS at atmospheric pressure. Moreover, it facilitated catalytic deoxygenation process through decarbonylation and decarboxylation processes, the Ni₂P phase's presence in catalyst was crucial in determining oxygen-removal efficiency and composition of liquid products. In order to produce

alkane and remove oxygen as efficiently as possible, Ni/P molar ratio and Ni loading amount that produced the largest volume fraction of Ni_2P phase in catalyst were 1.5 and 5.37 mmol/g Al_2O_3. In terms of deoxygenation reaction, catalytic activity of Ni_2P/Al_2O_3 catalysts was influenced by temperature and reaction conditions in addition to Ni_2P phase. The maximum output for liquid product (65.2 wt. %) is at 450°C with the catalyst 5.37-Ni_2P/Al_2O_3-1.5 with reaction time of 40 minutes. The RWS sample's oxygen atom content was reduced by > 85%, principally leading to creation of n-alkanes in diesel range (C_{15-19}). Optimal temperature was 450°C and gives optimum quantity of spent catalyst. Finally, author suggested that triglyceride hydrogenolysis and dehydration processes are key steps in deoxygenation process and provide an alternate solution to diesel engines.

Acknowledgements

References

Cecilia, J.A., Infantes-Molina, A., Sanmartín-Donoso, J., Rodríguez-Aguado, E., Ballesteros-Plata, D. and Rodríguez-Castellón, E. (2016), "Enhanced HDO activity of Ni 2 P promoted with noble metals", *Catalysis Sci. Technol.*, **6**(19), 7323-7333. https://doi.org/10.1039/C6CY00639F.

Chen, D., Ji, J., Jiang, Z., Ling, M., Jiang, Z. and Peng, X. (2020), "Molecular-confinement synthesis of sub-nano Fe/N/C catalysts with high oxygen reduction reaction activity and excellent durability for rechargeable Zn-Air batteries", *J. Power Sources*, **450**, 227660. https://doi.org/10.1016/j.jpowsour.2019.227660.

Peroni, M., Mancino, G., Baráth, E., Gutiérrez, O.Y. and Lercher, J.A. (2016), "Bulk and γ-Al2O3-supported Ni2P and MoP for hydrodeoxygenation of palmitic acid", *Appl. Catalysis B: Environ.*, **180**, 301-311. https://doi.org/10.1016/j.apcatb.2015.06.042.

Prins, R. and Bussell, M.E. (2012), "Metal phosphides: Preparation, characterization and catalytic reactivity", *Catalysis Lett.*, **142**(12), 1413-1436. https://doi.org/10.1007/s10562-012-0929-7.

Santillan-Jimenez, E., Loe, R., Garrett, M., Morgan, T. and Crocker, M. (2018), "Effect of Cu promotion on cracking and methanation during the Ni-catalyzed deoxygenation of waste lipids and hemp seed oil to fuel-like hydrocarbons", *Catalysis Today*, **302**, 261-271. https://doi.org/10.1016/j.cattod.2017.03.025.

Shrivastava, P., Kumar, A., Tekasakul, P., Lam, S.S. and Palamanit, A. (2021), "Comparative investigation of yield and quality of bio-oil and biochar from pyrolysis of woody and non-woody biomasses", *Energies*, **14**(4), 1092. https://doi.org/10.3390/en14041092.

Xin, H., Guo, K., Li, D., Yang, H. and Hu, C. (2016), "Production of high-grade diesel from palmitic acid over activated carbon-supported nickel phosphide catalysts", *Appl. Catalysis B: Environ.*, **187**, 375-385. https://doi.org/10.1016/j.apcatb.2016.01.051.

Zhao, Y.M., Zhang, P.C., Xu, C., Zhou, X.Y., Liao, L.M., Wei, P.J., Liu, E., Chen, H., He, Q. and Liu, J.G. (2020), "Design and preparation of Fe–N 5 catalytic sites in single-atom catalysts for enhancing the oxygen reduction reaction in fuel cells", *ACS Applied Materials & Interfaces*, **12**(15), 17334-17342. https://doi.org/10.1021/acsami.9b20711.

Zulkepli, S., Juan, J.C., Lee, H.V., Rahman, N.S.A., Show, P.L. and Ng, E.P. (2018), "Modified mesoporous HMS supported Ni for deoxygenation of triolein into hydrocarbon-biofuel production", *Energ. Convers.*

Manage., **165**, 495-508. https://doi.org/10.1016/j.enconman.2018.03.087.